THE JOURNAL OF PHYSICAL CHEMISTRY B

Article

pubs.acs.org/JPCB

On the Deactivation Mechanisms of Adenine−Thymine Base Pair

João Paulo Gobbo,*[,†] Vicenta Saurí,*[,‡] Daniel Roca-Sanjuán,*[,§] Luis Serrano-Andrés,[‡] Manuela Merchán,[‡] and Antonio Carlos Borin[†]

[†]Instituto de Química, Universidade de São Paulo, Av. Prof. Lineu Prestes 748, 05508-900 São Paulo, Brazil

[‡]Instituto de Ciencia Molecular, Universitat de València, P.B. Box 22085, 46071 València, Spain

[§]Department of Chemistry—Ångström, Theoretical Chemistry Program, Uppsala Univeristy, Box 518, 75120 Uppsala, Sweden

Supporting Information

ABSTRACT: In this contribution, the multiconfigurational second-order perturbation theory method based on a complete active space reference wave function (CASSCF/CASPT2) is applied to study all possible single and double proton/hydrogen transfers between the nucleobases in the adenine−thymine (AT) base pair, analyzing the role of excited states with different nature [localized (LE) and charge transfer (CT)], and considering concerted as well as step-wise mechanisms. According to the findings, once the lowest excited states, localized in adenine, are populated during UV irradiation of the Watson−Crick base pair, the proton transfer in the N−O bridge does not require high energy in order to populate a CT state. The latter state will immediately relax toward a crossing with the ground state, which will funnel the system to either the canonical structure or the imino−enol tautomer. The base pair is also capable of repairing itself easily since the imino−enol species is unstable to thermal conversion.

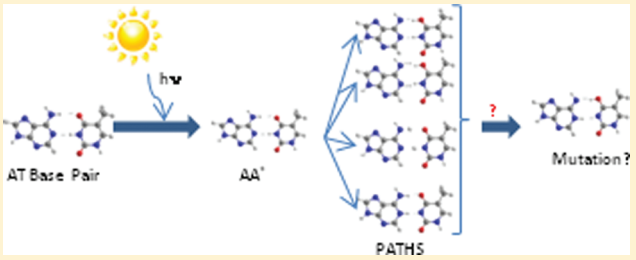

INTRODUCTION

DNA encodes the genetic information responsible for the development and functioning of living organisms. In a seminal work, Watson and Crick[1] proposed that the structure of DNA is composed by two nucleotide chains organized in double−helix manner around an axis, stabilized by hydrogen bonds formed between the canonical purine and pyrimidine bases: adenine−thymine (AT) and cytosine−guanine (CG). Therefore, the genetic code is stored in the form of hydrogen bonded nucleic acid bases. Nonetheless, it is known, nowadays, that external factors, like the presence of surrounding water molecules, also have a role in the stability and structure of the double helix.[2,3]

Alterations in DNA structure, if not repaired, may result in mutations, producing permanent change in the genetic code, or cell deaths. Among the mutagens, electromagnetic radiation, ultraviolet light (UV) in particular, is one of the most powerful damaging agents of DNA. During UV irradiation, biomolecules may be excited to a reactive electronic state, and the excess energy is then employed in photophysical or photochemical (radiative or nonradiative) processes. The formation of cyclobutane pyrimidine and pyrimidine 6−4 pyrimidone dimers, for instance, which may cause alterations in DNA replication and transcription, is one of the most common types of damage.[4−6]

To avoid undesired mutations, nature has developed nucleobases with very short excited−state lifetimes, which is known to be an intrinsic property of the isolated canonical nucleobases and is related to nonadiabatic processes that, ultimately, lead to the relaxation of the $^1\pi\pi^*$ excited states to the ground state, S_0.[7] Because of such extremely fast relaxation processes, usually in the femtosecond time scale, the excited species does not leave enough time to undergo chemical reactions.

Noncovalent interactions are the main cause of formation of aggregates between two or more nucleobases, which can be classified in two types: π-stacking (vertical) or hydrogen-bonded (horizontal) dimers. Those structural arrangements may open new paths for energy relaxation. In the vertically oriented π-stacking, for instance, the proximity of the aromatic molecules may facilitate the formation of excimers (excited dimers). The most striking feature of these excimers is the rising of long-lived emissive features not existent in the isolated nucleobases.[8] Because of their long lifetimes, they are supposed to be the key for intrastrand photolesions,[1,9−11] such as those cited above. A study of the excited-state dynamics of AT base pair suggests that the excited oligo- and polynucleotides decay from a localized $^1\pi\pi^*$ to an excimer-like state with high quantum yield, explaining why most lesions involve stacked pairs.[12]

The interstrand proton or hydrogen transfer reaction between two nucleobases in the horizontal hydrogen-bonded arrangement can lead to the formation of rare zwitterionic or imino−enol tautomers. Despite this type of DNA damage happens less frequently than that caused by excimers,[12] Löwdin[13,14] suggested that if the rare tautomers have a lifetime longer than the time needed to open and replicate the DNA strand, simultaneous mutations in both DNA strands may occur. Several experimental studies with a model compound (7-azaindole

Received: January 17, 2012
Revised: March 13, 2012
Published: March 13, 2012

   dx.doi.org/10.1021/jp300583h | J. Phys. Chem. B 2012, 116, 4089−4097

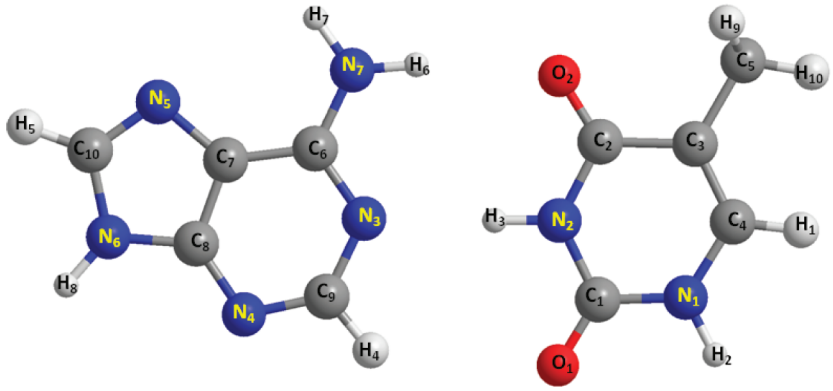

Figure 1. Atom labeling and numbering for the adenine−thymine base pair.

dimer) discussing the dynamics and the mechanism of the process have been published,[15−18] as well as theoretical predictions proposing two static stepwise mechanisms based on the presence of a neutral and an ionic intermediate after a proton being transferred from one moiety to the other.[19]

Several authors have tried to explain the formation of the imino−enol tautomer, discussing the energetics and the equilibrium geometries involved in the proton transfer reaction, as well as the characterization of the transition state in the ground state canonical base pair.[20−25] A seminal work on the photophysical and photochemical properties of the adenine−thymine base pair was published by Perun et al.,[26] who proposed that after the excitation to a locally excited state ($^1\pi\pi^*$−LE) on adenine, a conical intersection (CI) connecting the LE to a charge transfer excited state ($^1\pi\pi^*$−CT) is readily accessible. Once in the CT state, the system evolves in a barrierless manner toward another CI crossing, this time with the ground state, S_0, by means of a proton transfer from adenine to thymine in the N(A)−H···O(T) bridge. Ai et al.[27] discussed the convenience of using the 2-aminopyridine pair as a model to analyze the CT state in the AT base pair. On the basis of density functional theory (DFT) calculations, employing the CAM-B3LYP functional, the authors supported the idea that, in the excited state $^1\pi\pi^*$, the proton will move from adenine to thymine triggered by the charge separation obtained after excitation, as previously studied.[26]

Despite the proton or hydrogen transfer reaction in the excited state of the AT base pair has been an active area of interest in the past decade,[20−27] there are still some open questions to debate, as for instance, the precise structure of the CI between the CT and ground states, the mechanisms for zwitterionic and imino−enol tautomers formation, and the energy-decay paths and intermediate species responsible for the photostable properties of AT. The aim of the present work is to describe the proton/hydrogen photochemical processes by using multiconfigurational methods in terms of optimized geometries and potential energy hypersurfaces (PEHs) connecting the most relevant points, as well as to discuss the most important mechanisms for deactivation that may lead the system back to its former equilibrium structure or to a rare tautomer.

METHODOLOGY

Geometry optimizations and PEH crossing-point (CIs) computations were performed initially at the complete-active-space self-consistent-field (CASSCF) level of theory.[28] The most relevant structures were connected via linear interpolation in internal coordinates (LIIC). For each computed geometry, dynamic correlation effects were introduced by means of multiconfigurational second-order perturbation theory (CASPT2)[29,30] single-point calculations, with the standard zeroth-order Hamiltonian. This strategy (the CASPT2//CASSCF protocol) has been successfully used in other applications with similar molecular systems.[6,7,11,31] No IPEA shift[32] (ionization potential−electron affinity shift) was used and intruder states problems were handled with an imaginary shift[33] of 0.2 au. The atomic natural orbital (ANO-L)[34] basis set of double-ζ quality plus polarization were used, being described as C,N,O(10s6p3d)/H(7s3p) primitive Gaussian functions contracted to C,N,O[3s2p1d]/H[2s1p]. All calculations were performed in the C_s point-group symmetry, with an active space comprising 12 electrons distributed among 12 orbitals belonging to the a'' irreducible representation (six π and six π^* orbitals). The MOLCAS-7.4 package of software was employed.[35] Cartesian coordinates for the structures discussed in this article can be found at the Supporting Information.

RESULTS AND DISCUSSION

Stationary Points. Figure 1 displays the atom numbering used in this work. The structures of the relevant stationary points of the Watson−Crick and imino−enol tautomers computed for the ground state and the excited−state intermediates of AT base pair are displayed in Figure 2; the corresponding selected bond lengths together with some results published previously are listed in Table 1. Vertical transition energies and dipole moments for the canonical and imino−enol tautomers are compiled in Tables 2 and 3. The relative energies reported in the tables and in the full article are referred to the ground-state energy at the Watson−Crick geometry.

Watson−Crick Tautomer. The optimized ground state intramolecular bond lengths for both nucleobases in the AT base pair are consistent with previous results obtained at different levels of theory, differing by no more than 0.07 Å (see Table 1). Regarding the intermolecular hydrogen-bond distances, for which a qualitative agreement with other studies was obtained, the computed distance between the N atoms in the N_2−N_3 bridge (3.04 Å) of AT pair is shorter than the N_7−O_2 bond length (3.22 Å). As expected, our results are closer to those reported by Guallar et al.[21] and Shukla and Leszczynski;[22] our CASSCF calculations encompass only π orbitals in the active space, while the inactive σ orbitals should resemble the corresponding Hartree−Fock canonical orbitals.

Table 2 compiles the present computed vertical transition energies and dipole moments, together with other theoretical results selected from the literature. The S_1 and S_2 excited states are placed, respectively, at 4.74 and 4.80 eV above the ground

dx.doi.org/10.1021/jp300583h | J. Phys. Chem. B 2012, 116, 4089−4097

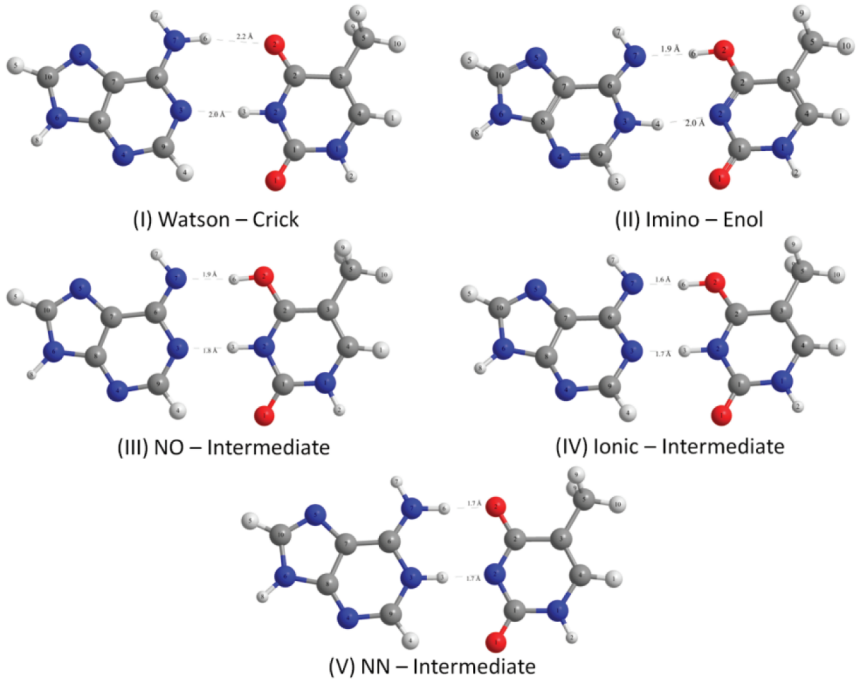

Figure 2. Scheme of the structures for the most relevant stationary points in the photochemistry of adenine−thymine base pair.

Table 1. Selected Bond Distances (Å) for Watson−Crick, Imino−Enol Tautomer, NO−Intermediate, Ionic−Intermediate, and NN−Intermediate Geometries

	N_7-H_6	N_7-C_6	C_6-N_3	C_2-O_2	C_2-N_2	N_2-H_3	H_6-O_2	N_3-H_3	N_2-N_3	N_7-O_2
					Watson−Crick					
this work	1.00	1.35	1.33	1.21	1.38	1.01	2.24	2.03	3.04	3.22
ref 20[a]	1.07					1.10	1.73	1.65	2.74	2.80
ref 21[b]	1.00					1.02	2.02	1.86	2.88	3.02
ref 22[c]		1.33	1.33	1.21	1.38		2.09	2.01	3.02	3.09
ref 23[d]	1.03					1.06	1.90	1.78	2.84	2.92
ref 26[e]		1.35	1.35	1.24	1.39		1.93	1.77		
ref 27[f]	1.02	1.34	1.35	1.24	1.39	1.05	1.92	1.80	2.85	2.94
					Imino−Enol					
this work	1.86	1.28	1.39	1.31	1.29	2.05	0.97	1.00	3.03	2.82
ref 20[a]	1.47					1.57	1.11	1.11	2.68	2.58
ref 23[d]	1.44					1.69	1.11	1.06	2.75	2.55
ref 27[f]	1.44	1.30	1.39	1.30	1.33	1.70	1.10	1.06	2.76	2.56
					NO−Intermediate					
this work	1.89	1.30	1.38	1.31	1.36	1.02	0.97	1.79	2.80	2.85
					Ionic−Intermediate					
this work	1.63	1.35	1.35	1.27	1.33	1.05	1.00	1.67	2.72	2.63
ref 21[b]	2.03					1.02	0.99	1.93		
					NN−Intermediate					
this work	1.04	1.32	1.39	1.24	1.33	1.69	1.66	1.00	2.69	2.70

[a]HF/MINI-1. [b]HF(S_0)-CIS/6-31G. [c]HF(S_0)-CIS/6-31++G(d,p). [d]B3LYP/cc-pVDZ. [e]MP2/cc-pVDZ. [f]TD-DFT/6-31G(d,p).

state and correspond to localized excitations on the adenine moiety (AA*). Next, a locally excited state on thymine (TT*) is found at 5.65 eV above the ground state. Despite the different energy range values shown in Table 2, derived from the use of different methods, it is clear that there are at least three locally excited states (LE) (two AA* and one TT*) below the CT state (AT*).

The S_1 state (LE−AA*) is characterized by a single excitation involving the natural orbitals 6 and 8 in the active space (6 → 8, Figure 3) and shows an alternation of bonding to antibonding orbitals in the adenine moiety. It can be traced back to the ^1L_a ($\pi\pi^*$) excited state of adenine.[36] Almost degenerate to S_1 (ΔE = 0.06 eV), the S_2 excited state has a wave function dominated by two singly excited configurations (6 → 8 and 4 → 8) with basically the same weight; both represent a LE state on adenine. According to our CASPT2 results, these LE states on adenine are red-shifted in the AT base pair with respect to previous results obtained for the isolated monomer.[36] The first LE state of TT* type, also with a wave function dominated by a single configuration, involving the electronic excitation 5 → 7, S_3, is located vertically at 5.65 eV above the S_0, in agreement with the values reported by Domcke and co-workers.[26] Our results

dx.doi.org/10.1021/jp300583h | J. Phys. Chem. B 2012, 116, 4089−4097

Table 2. Vertical Transition Energy (ΔE, eV) and Dipole Moments (μ, D) for the Lowest Singlet $\pi\pi^*$ States in the Watson–Crick Geometry of Adenine–Thymine Base Pair

		ΔE (eV)					
state	transition		ref 22	ref 26	ref 27	ref 36[a]	μ (D)
GS		0.00	0.00	0.00	0.00	0.00	2.37
S_1	A → A*	4.74	6.39	5.45	5 0.48	5.35	5.28
S_2	A → A*	4.80	6.52	5.25		5.16	2.94
S_3	T → T*	5.65	6.49	5.37		4.89	5.57
S_4	A → A*/ A → T*	5.72					5.52
S_5	A → T*	6.08	7.22	6.26	5.85		13.61
S_6	A → A*	6.27					3.55

[a]Isolated nucleobase.

Table 3. Vertical Transition Energy (ΔE, eV), Total Charge on the Thymine Moiety, and Dipole Moments (μ, D) for the Lowest Singlet $\pi\pi^*$ States of the Imino–Enol Tautomer

state	transition	ΔE	charge	μ
GS		0.62	−0.03	2.94
S_1	A → A*	4.93	−0.03	5.65
S_2	A → A*	5.49	−0.12	1.15
S_3	T → T*	5.86	−0.02	6.61
S_4	A → T*	6.16	−0.80	17.50
S_5	A → A*	6.30	−0.12	2.62
S_6	A → A*	6.75	−0.06	3.44

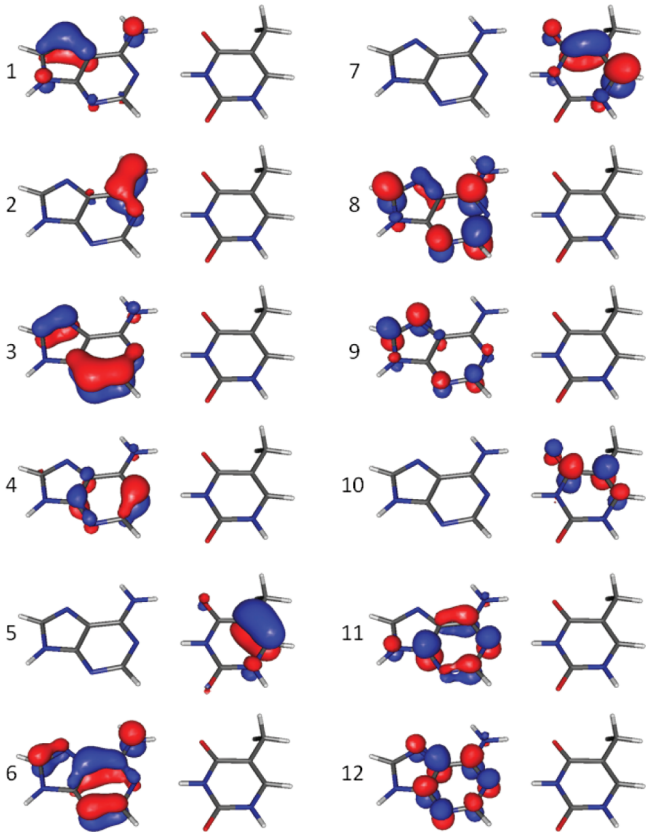

Figure 3. Most important π natural orbitals of adenine–thymine base pair in the Watson–Crick geometry.

suggest that the TT* state is blue-shifted after pairing with adenine.

The vertical lowest lying CT excited state of the AT base pair, at 6.08 eV above the ground state (Table 2), represents an excitation from a bonding orbital localized on the adenine moiety to an antibonding orbital localized on thymine (AT*, 6 → 7). Because of its intrinsically ionic character, it has the greatest dipole moment of all states computed in this work, 13.6 D (cf. Table 2). Shukla and Leszczynski[21] suggested the existence of two CT states for AT and cytosine–guanine base pair in an accessible energetic region, at 7.22 and 7.09 eV, respectively. The authors also reported the dipole moments for these states as 4.68 and 3.99 D, respectively, a bit lower than what would be expected for an excited state of CT nature. The results from Domcke and co-workers[26] and Ai et al.[27] place the CT state in a not so high energetic region (~6 eV), with a much larger dipole moment (>10 D), in agreement with the present computed values (see Table 2).

In order to estimate the quality of our results, test calculations were carried out with the restricted active space second-order perturbation theory (RASPT2) method,[37] from which the vertical excitation energies of the $^1n\pi^*$ excited states were also computed. In short, all π space of the adenine–thymine base pair plus two lone pairs were included in the calculation performed within the constraints of C_s symmetry. For the singlet a'' ($\pi\pi^*$) states, calculations were carried out with a RAS1/RAS3 space of 12/7 orbitals, allowing a maximum of quadruple excitations, as recommended in previous works.[37,38] For the singlet a' ($n\pi^*$) electronic states, the lone pair n orbitals were added in the active space. The results for the CT and the adenine LE states computed at the RASPT2 level are in excellent agreement with those obtained with the CASPT2 method (less than 0.1 eV). Nonetheless, a larger discrepancy is observed for the electronic states localized in thymine, for which the RASPT2 results point out to a very small energetic gap between the S_1 and S_2 states. As to the $^1n\pi^*$ excited states, the first of them, located vertically at 4.9 eV above the ground state, was identified as been of TT* type, followed by one of AA* type at 5.33 eV. It is worth mentioning that our computed $^1n\pi^*$ excited states appear in the same energetic region as reported by Perun et al.,[26] but in contrast to them, the lowest $^1n\pi^*$ excited state computed here does not carry any contribution from the lone pair orbital of adenine, being fully localized on the thymine moiety.

Imino–Enol Tautomer. Despite the differences noted for the selected bond distances obtained with different methods (cf. Table 1), one can conclude that for the imino–enol tautomer, the two moieties approach each other with a relative rotation of the two monomers since the N_3–N_2 distance is similar to that observed for the Watson–Crick structure but that the N_7–O_2 distance is shorter. The ground (S_0) state of the imino–enol tautomer is located vertically at 0.62 eV above the ground state minimum (see Table 3) of the Watson–Crick structure, in agreement with the values published by Villani[23] (0.56 eV) and Florián et al.[20] (0.40 eV).

As observed for the Watson–Crick structure in the Franck–Condon region, the three lowest-lying excited states of the imino–enol tautomer have AA* [4.93 eV (S_1) and 5.49 eV (S_2)] and TT* [5.86 eV (S_3)] character (Table 3). Whereas the S_1 and S_2 states in the Watson–Crick structure are almost degenerate, they appear with a relatively larger separation in the imino–enol tautomer (ΔE = 0.56 eV). The CT state (AT*) is located in the same energetic region as for the Franck–Condon counterpart (6.16 eV), with a computed dipole moment of 17.5 D.

NO–Intermediate. As shown schematically in Figure 4, after irradiation with UV light, a proton/hydrogen transfer can occur

dx.doi.org/10.1021/jp300583h | J. Phys. Chem. B 2012, 116, 4089–4097

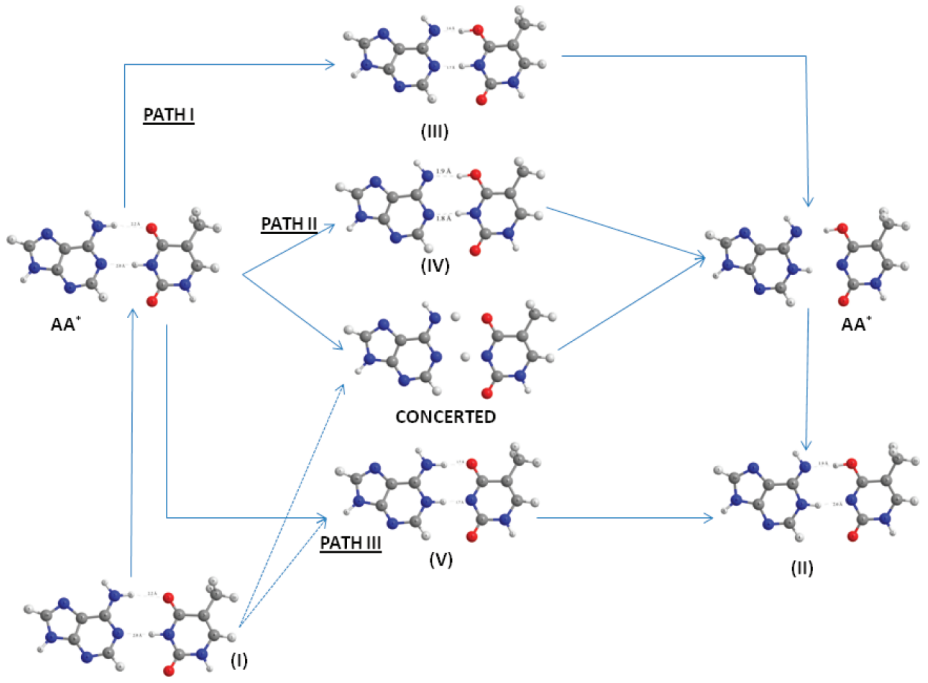

Figure 4. Scheme of photochemical deactivation mechanisms in adenine−thymine base pair. The dotted arrows means that the reaction was also studied in the S_0 hypersurface.

in the excited state, involving the $N_7-H_6-O_2$ bridge via two different mechanisms (Figure 4), as shall be discussed in detail below. The first one is related to a non-adiabatic process through a CI with the ground state and involves a CT state A → T*, $(S_0/CT)_{CI}$. Because of the charge separation taking place in the CT state (A → T*), the transfer of a proton in the excited state is extremely favored, to the point that the PEH of the excited state crosses the ground state surface, as suggested by Domcke et al.[26]

The minimum of the CT excited state, the NO−intermediate, is located around a CI region $(S_0/CT)_{CI}$ at 2.4 eV above the Watson−Crick S_0 equilibrium geometry. It is possible to describe the electronic structure of this point as the linear combination of two configurations: the corresponding ground-state-like closed-shell and the CT configurations. The decrease of charge separation due to the proton transfer in the N−O bridge is reflected in a smaller dipole moment (2.90).

In comparison with the Franck−Condon region of the Watson−Crick structure, the nucleobase moieties become closer to each other, as shown by the shorter N_7-O_2 and N_2-N_3 bond lengths in Table 1 (3.22 and 3.04 Å, respectively, for the optimized Watson−Crick conformer against 2.85 and 2.80 Å, respectively, for the optimized geometry of NO−intermediate). Perun et al.[26] proposed that in order to reach the CI region, the separation between adenine and thymine moieties must increase up to a distance of 2.8 Å for the N_7-H_6 bond, whereas in our calculation, the CI crossing is located at shorter bond lengths (1.9 Å).

Ionic−Intermediate. The other mechanism for proton/hydrogen transfer in the N−O bridge involves an ionic intermediate and takes place in a LE state on adenine. After absorption of UV radiation, if the electron remains localized in this nucleobase throughout the proton−transfer process, an ionic system with positive charge on thymine and negative on adenine is generated. In contrast to the scenario for the NO−intermediate, showing a CI with the ground state, the ionic path leads to a shallow minimum in the PEH of the CT state (3.96 eV).

Because of the charge separation, as the proton is transferred from one moiety to the other, the distances between adenine and thymine becomes smaller in the ionic−intermediate structure in comparison to the $(CT/gs)_{CI}$ geometry (see Table 3); for instance, the N_7-O_2 bond distance decreases from 2.85 Å to 2.63 Å (Δd = 0.22 Å), while the N_2-N_3 bond length is 0.08 Å shorter. As the N_7-O_2 separation decreases much more than N_2-N_3, an in-plane rotation of the monomers takes place.

NN−Intermediate. The last possibility studied by us concerns the hydrogen transfer from thymine to adenine in the N_2-N_3 bridge. The moieties also tend to become closer in comparison with the Watson−Crick structure, shortening the N_7-O_2 bond distances from 3.22 to 2.70 Å and from 3.04 to 2.69 Å in the N_2-N_3 bridge. That means differences of 0.52 and 0.35 Å, much larger than those corresponding to the other intermediates and imino−enol tautomer. The remaining distances are kept as in the Watson−Crick region.

The ground state of the NN−intermediate is placed at 0.45 eV above the Watson−Crick structure. The lowest excited state is of AA* type and has a relative energy of 4.39 eV. The lowest CT state computed at this geometry appears in a much higher energetic region (6.23 eV) and will not be discussed further.

Until now we have described the reactants, intermediates, and products of proton/hydrogen transfer reactions in the AT base pair. In the next section, several paths connecting these stationary points that, as a final consequence, may result in DNA damage or restore the initial structure are analyzed. We are concerned on the decay routes involving a transfer of a proton or hydrogen from one nucleobase to the other, although it is worth keeping in mind that the deactivation paths of the isolated nucleobases might also be possible.

Reaction Paths. Four possible photochemical paths involving proton/hydrogen transfer in the AT base pair are discussed in this section: one concerted (double proton transfer reaction) and three step-wise processes (proton/hydrogen transfer reaction), occurring via the N−O (two) and N−N (one)

dx.doi.org/10.1021/jp300583h | J. Phys. Chem. B 2012, 116, 4089−4097

bridges. Ground- and excited-state PEHs have been mapped along these routes between the optimized reactants, intermediates, and products involved in each path (see Figures 5–8). The

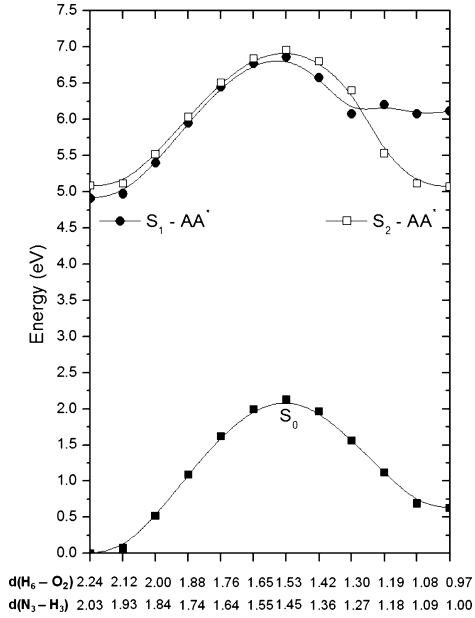

Figure 5. AT base pair potential energy hypersurfaces of the ground and low-lying excited S_1 and S_2 states mapped at the CASPT2 level along the O_2–H_6 and N_3–H_3 reaction coordinates in Angstroms between the Watson–Crick canonical structure (left) and the imino–enol tautomer (right), via the concerted pathway.

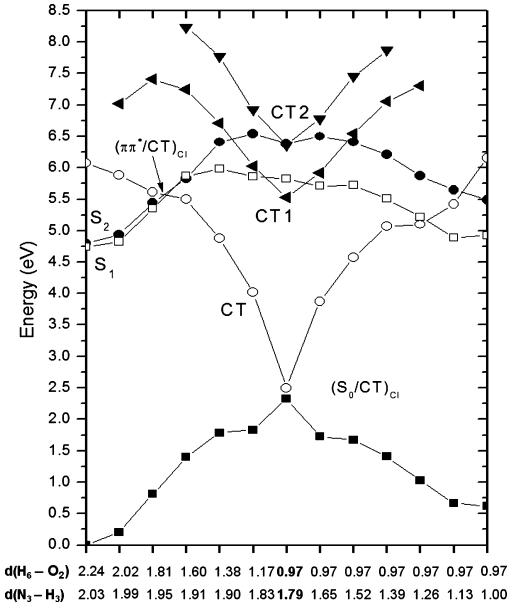

Figure 6. AT base pair potential energy hypersurfaces of the ground and five low-lying excited states (S_1, S_2, CT, CT1, and CT2) mapped at the CASPT2 level along the O_2–H_6 and N_3–H_3 reaction coordinates in Angstroms between the Watson–Crick canonical structure (left), the NO–intermediate (middle), and the imino–enol tautomer (right), via PATH I.

O_2–H_6 and N_3–H_3 distances, corresponding to the hydrogen bonds in AT, are used to monitor the evolution of the photochemical events.

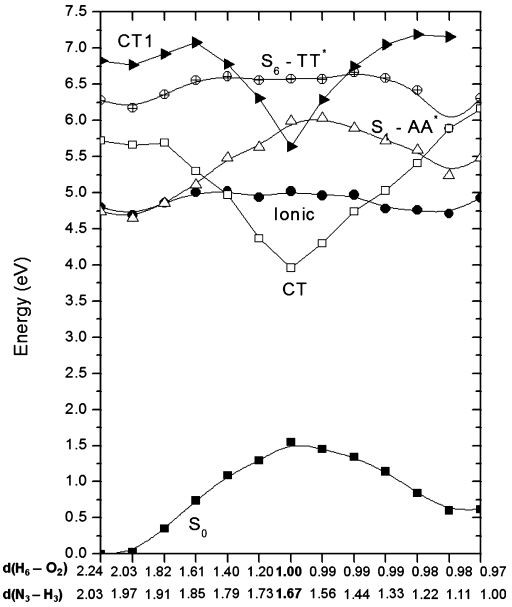

Figure 7. AT base pair potential energy hypersurfaces of the ground and five low-lying excited states (S_1, ionic, CT, S_6, and CT1) mapped at the CASPT2 level along the O_2–H_6 and N_3–H_3 reaction coordinates in Angstroms between the Watson–Crick canonical structure (left), the ionic–intermediate (middle), and the imino–enol tautomer (right), via PATH II.

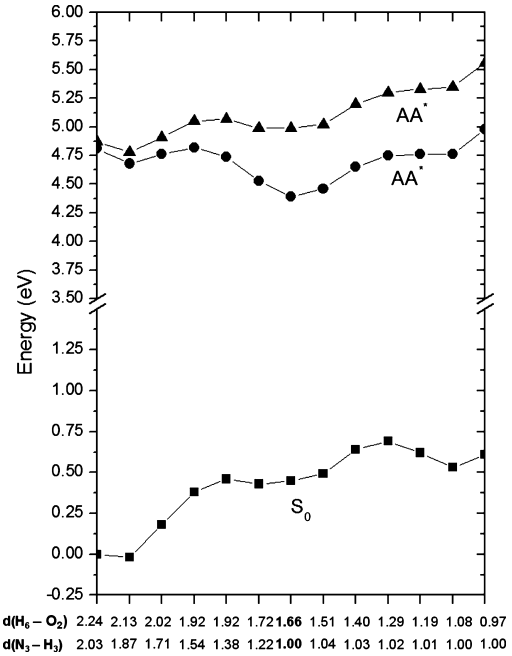

Figure 8. AT base pair potential energy hypersurfaces of the ground and low-lying excited S_1 and S_2 states mapped at the CASPT2 level along the O_2–H_6 and N_3–H_3 reaction coordinates in Angstroms between the Watson–Crick canonical structure (left), the NN–intermediate (middle), and the imino–enol tautomer (right), via PATH III.

Guallar et al.[21] considered the formation of the rare imino–enol tautomer on the canonical base pairs at the Hartree–Fock and configuration interaction singles (CIS) levels of theory. For the concerted double proton transfer reaction in the ground state, they concluded that a very high energetic

dx.doi.org/10.1021/jp300583h | J. Phys. Chem. B 2012, 116, 4089–4097

barrier (22.51 kcal·mol^{-1}) must be surmounted in order to reach the imino−enol region. As explained by the authors, this tautomer is not stable since the reverse path is basically barrierless. In addition, it was suggested that the energy barrier for this mechanism could be much smaller in the excited states.

Villani[23−25] tried to explain the formation of the imino−enol tautomer employing two and four dimensional models to describe the ground−state PEH. In short, it was proposed that the hydrogen atom moves in a concerted way in the N−O bridge and two diabatic states are involved, while the mechanism is step-wise in the N−N bridge, and just one diabatic state is necessary for its description.

We expand here the study including the excited states of AT base pair, analyzing both the thermal and photochemical reactivity at the CASSCF/CASPT2 level of theory. First, the concerted relaxation mechanism will be discussed (see Figure 5). Several electronic-state PEHs were explored between the Watson−Crick structure at the Franck−Condon (I) geometry and the imino−enol region (II). As can be deduced from Figure 5, the concerted path is not likely for all the states because it would be necessary to overcome a large energetic barrier (up to 2 eV), in order to reach the imino−enol tautomer region. The same behavior was observed by other authors[20,23−25] at different levels of theory.

The PEHs connecting the Watson−Crick structure and the NO−intermediate (PATH I) is shown in Figure 6. As the proton moves from adenine to thymine and the O_2−H_6 distance becomes shorter, the energies of the ground and the lowest lying excited states (S_1 and S_2) increase. In turn, the energy of the lowest CT state decreases, and as a consequence, this state crosses first with the S_2 and S_1 hypersurfaces and finally reaches the $(S_0/CT)_{CI}$ in the region of the NO−intermediate. Several other CT states exist,[26,27] but they are higher in energy and therefore will not be further discussed. The opposite trend is observed as the system evolves from the intermediate region to the rare tautomer equilibrium structure, with a second exchange of H atom between the base pair nucleobases (in this case via the N−N bridge). Hence, the LE states are stabilized and the CT states destabilized in this part of the energy profile.

As can be observed in Figure 6, the initially populated AA* states at the Franck−Condon region of the Watson−Crick structure needs to cross the CT state $[(LE/CT)_{CI}]$ before reaching the $(S_0/CT)_{CI}$ crossing. Ai et al.[27] pointed out that the barrier height depends strongly on the hydrogen-bond lengths. Taking into account that our CASSCF optimizations overestimate the distance between the two nucleobases (see Table 1) and considering the limitations of the strategy employed to explore the PEHs between reactants, intermediates, and products, the barrier depicted in Figure 6 must be understood as an upper limit to the real difference energy. Indeed, other evidence indicate a lower value.[26,27] A relevant conclusion is obtained from our results for the photochemical process: in the vicinity of the AA* electronic excited states of the canonical Watson−Crick base pair populated during the UV irradiation, the hydrogen bonded dimer can reach the CT state and subsequently decay in a barrierless manner toward the $(S_0/CT)_{CI}$ point.

Another interesting aspect is the even lower barrier for the corresponding $(LE/CT)_{CI}$ crossing in the imino−enol region from which we can infer that there is a more accessible path for the tautomer in the excited state manifold (with respect the canonical base pair) bringing the system back to its ground state minimum or to the restored Watson−Crick AT pair.

The photochemical route connecting the canonical AT structure and the imino−enol tautomer via the ionic−intermediate has been called PATH II (Figure 7). As in PATH I, it is related to a step-wise process in which the first proton transfer takes place through the N−O bridge. As can be seen in Figure 7, once the LE state is reached during UV irradiation of the canonical AT, the system may evolve to the ionic−intermediate region after overcoming a very small energetic barrier.

The PATH II trends are quite similar to those observed in PATH I, in general, but the CT states are not so stabilized. Therefore, when the proton is fully transferred, there is a considerable gap of about 2.5 eV between the S_0 and the lowest CT state (AT*). Contrary to what happens in PATH I, for which the proton transfer to thymine neutralizes the charge separation observed in the CT excited state, in PATH II, the initially populated excited state is localized in the nucleobase, and the movement of the proton causes a charge separation between the two moieties. Although the state optimized in the ionic−intermediate is the localized AA* excitation, the CT state is lower in energy at this point and can be easily populated through the $(LE/CT)_{CI}$ crossing. Indeed, the fact that the barrier to reach the $(LE/CT)_{CI}$ structure is lower in PATH II than in PATH I may have mechanistic and dynamic consequences. Dynamics calculations on the excited states of the dimer will be of great help to elucidate which mechanism is favored, which is challenging for the current methodologies because of the size of the molecular system. At the $(LE/CT)_{CI}$ point, the system may proceed on the LE state hypersurface, leading to the enol−imino form in the excited state, or may decay to the CT state. The vibrational relaxation of the latter will drive the system to the $(S_0/CT)_{CI}$ found in PATH I. Although this photochemical route is not mentioned by Perun et al.,[26] we believe, in agreement with Ai et al.,[27] that it is extremely important to describe this nonradiative decay channel.

The last path described in this work concerns the N−N bridge (PATH III, see Figure 8) on which the first proton transfer occurs from thymine to adenine, i.e., in opposite direction to PATHS I and II. As can be seen in Figure 8, the ground-state PEH does not exhibit high energy barriers between the canonical and imino−enol species, other than the energy difference between both AT structures, suggesting that the thermal reaction for tautomer production should happen via this path or in a parallel one. It may also be suggested that the reverse path restoring the canonical base pair may occur without any significant energetic barrier. As it will be pointed out later, this fact will have important consequences in the global photochemical scheme.

The hypersurfaces of the two lowest lying LE (AA*) states have a very small energetic barrier to reach the NN−intermediate, which is localized in a shallow minimum. The PEHs plotted for PATHS II and III (Figures 7 and 8, respectively) suggest that the hydrogen atoms in both bridges (N−O and N−N) may move relatively free in the excited state toward the complementary nucleobase. Because of this degree of freedom, the paths to the crossing region $(LE/CT)_{CI}$ may be accessible, which would enhance the fast radiationless deactivation mechanisms via the $(S_0/CT)_{CI}$, avoiding damaging the genetic material. It suggests also that nature has developed several regenerative paths, either in the ground or excited states, to restore the imino−enol tautomer via any of the previous described mechanisms to the canonical structure. Our findings for the path involving the NN−intermediate and those reported by Ai et al.[27] represent different possibilities. The crossing between

dx.doi.org/10.1021/jp300583h | J. Phys. Chem. B 2012, 116, 4089−4097

the low lying $^1\pi\pi^*$ excited state and the CT state of T →A nature has not been found in the present study since it is located too high in energy (~6.23 eV) at our optimized NN− intermediate geometry.

As the mechanistic pictures presented until now represent cuts on the hypersurfaces computed with the CASSCF/CASPT2 method, an integration of the three paths may lead a more comprehensive description of the photochemistry of the AT base pair. Starting at the LE state on adenine, the hydrogen atoms in the hydrogen bonds of the AT base pair become prone to be transferred between the moieties. The more likely path, at the beginning at least, in the N−O bridge should be PATH II, which exhibits a lower barrier in the PEH (Figures 6 and 7) associated to the proton transfer from adenine to thymine. Before reaching the ionic−intermediate, the system passes through the $(LE/CT)_{CI}$ region, from where most of the population may be transferred to the CT state. Next, the base pair may proceed in this state from the ionic−intermediate region to the crossing with the ground state described in PATH I $[(S_0/CT)_{CI}]$, decaying to S_0. However, if the system has initially enough excess of energy to overcome the first barrier in PATH I, the $(LE/CT)_{CI}$ crossing may also be reached via this path and AT would evolve directly to the NO−intermediate region and to the $(S_0/CT)_{CI}$. The height of the barrier the system needs to surmount to reach the $(LE/CT)_{CI}$ seam in PATHs I and II deserve special attention. This height will ultimately determine the way that the system will most probably take to become deactivated. According to the results obtained in our CASSCF/CASPT2 calculations, we estimate 0.75 and 0.25 eV as upper bounds for the energy barriers to reach the CI along PATHS I and II, respectively.

Finally, once the imino−enol tautomer is formed in the excited state, the canonical base pair may be regenerated in the excited states through PATHs I, II, and III. In case the tautomer reaches its ground-state equilibrium structure, it finds in PATH III a barrierless decay to restore the canonical base pair. Molecular dynamics studies are necessary to ultimately estimate how long the system will remain in the imino−enol tautomer form, but our results confirm once more the complexity and formidable efficiency of the photophysical deactivation mechanisms available in our genetic material.

CONCLUSIONS

The CASSCF/CASPT2 method has been used to describe the deactivation photochemical paths of adenine−thymine base pair, which follow UV irradiation and involve proton/hydrogen transfer processes between both nucleobases. All relevant proton/hydrogen exchanges, concerted and step-wise mechanisms, and excited states of different nature (LE and CT states) have been considered in order to provide with a general description of the photochemistry of AT base pairs. The present results, together with previous results on the decay paths found in isolated nucleobases[7] and the production of lesions in π-stacked pyrimidine molecules[6,11] contribute to the understanding of the photochemistry and photoreactivity of DNA.

In short, after light incidence, the bright AA* state is populated and new deactivation channels become accessible, in addition to the ultrafast decay paths present in isolated nucleobases. As found in the present study, there are at least three additional paths in which the system may evolve: two involving the N−O bridge (PATHS I and II) and one taking place via the N−N bridge (PATH III). Our results show that PATHS I and II lead the system to a CI crossing with the ground state, $(S_0/CT)_{CI}$, which mediates the decay of the system toward the canonical Watson−Crick structure or to the production of an imino−enol tautomer. In PATH III, the excited-state PEHs between the canonical AT and the tautomer are flat, and the latter can be reached as well in the excited state.

Although these photochemical routes favor the formation of the imino−enol tautomer, we found also several possible paths that regenerate the system back to the canonical adenine−thymine base pair. The reverse routes of PATHS I, II, and III, involving photoexcitation of the tautomer, are strong candidates for this regeneration. In addition, according to the ground-state energy profile from the tautomer to the Watson−Crick AT base pair through the NN-intermediate, the imino-enol system is unstable to thermal conversion to the canonical base pair.

ASSOCIATED CONTENT

Supporting Information

Cartesian coordinates of the optimized structures. This material is available free of charge via the Internet at http://pubs.acs.org.

AUTHOR INFORMATION

Corresponding Author

*E-mail: jpgobbo@iq.usp.br (J.P.G.); Vicenta.Sauri@uv.es (V.S.); Daniel.Roca@kvac.uu.se (D.R.-S.).

Notes

The authors declare no competing financial interest.

ACKNOWLEDGMENTS

J.P.G. acknowledges FAPESP and CAPES for a financial support. We acknowledge CTQ2007-61620, CTQ2010-14892, and CSD2007-0010 Consolider Ingenio in Molecular Nanoscience of the Spanish MICINN/FEDER and the Generalitat Valenciana. D.R.S. also thanks the European Research Council under the European Community's Seventh Framework Programme (FP7/2007-2013)/ERC grant agreements no. 255363. A.C.B. acknowledges continuous academic support from CNPq (Conselho Nacional de Desenvolvimento Científico e Tecnológico), FAPESP (Fundação de Amparo à Pesquisa do Estado de São Paulo), and the services and computer time at the Laboratório de Computação Científica Avançada (LCCA) of the Universidade de São Paulo.

REFERENCES

(1) Watson, J.; Crick, F. *Nature* **1953**, *171*, 964.
(2) Rueda, M.; Kalko, S.; Luque, F.; Orzoco, M. *J. Am. Chem. Soc.* **2003**, *125*, 8007.
(3) Rueda, M.; Luque, F.; Orzoco, M. *J. Am. Chem. Soc.* **2006**, *128*, 3608.
(4) Cadet, J.; Vigny, P. In *Bioinoriganic Photochemistry*; Morrison, H., Ed.; John Wiley & Sons: New York, 1990.
(5) Douki, T.; Cadet, J. *Biochemistry* **2001**, *40*, 2495.
(6) Roca-Sanjuán, D.; Olaso-González, G.; González-Ramirez, I.; Serrano-Andrés, L.; Merchán, M. *J. Am. Chem. Soc.* **2008**, *130*, 10768.
(7) Serrano-Andrés, L.; Merchán, M. *J. Photochem. Photobiol. C* **2009**, *10*, 21.
(8) Crespo-Hernández, C. E.; Cohen, B.; Hare, P. M.; Kohler, B. *Chem. Rev.* **2004**, *104*, 1977.
(9) Pechenaya, V. I.; Danilov, V. I.; Slyusarchuk, V. N.; Alderfer, J. L. *Photochem. Photobiol.* **1995**, *61*, 435.
(10) Danilov, V. I.; Slyusarchuk, V. N.; Alderfer, J. L.; Stewart, J. P. P.; Callis, P. R. *Photochem. Photobiol.* **1994**, *59*, 125.

(11) González-Ramirez, I.; Roca-Sanjuán, D.; Climent, T.; Serrano-Pérez, J. J.; Merchán, M.; Serrano-Andrés, L. *Theor. Chem. Acc.* **2011**, *128*, 705.
(12) Crespo-Hernández, C. E.; Cohen, B.; Kohler, B. *Nature Lett.* **2005**, *436*, 1141.
(13) Löwdin, P. O. *Rev. Mod. Phys.* **1963**, *35*, 724.
(14) Löwdin, P. O. *Adv. Quantum Chem.* **1965**, *2*, 213.
(15) Douhal, A.; Kim, S. K.; Zewail, A. H. *Nature* **1995**, *378*, 260.
(16) Chou, P. T.; Yu, W.-S.; Chen, Y.-C.; Wei, C.-Y.; Martinez, S. S. *J. Am. Chem. Soc.* **1995**, *120*, 12927.
(17) Kwon, O.-H.; Zewail, A. H. *Proc. Natl. Acad. Sci. U.S.A.* **2007**, *104*, 8703.
(18) Sekyia, H.; Sakota, K. *J. Photochem. Photobiol., C* **2008**, *9*, 81.
(19) Serrano-Andrés, L.; Merchán, M. *Chem. Phys. Lett.* **2006**, *418*, 569.
(20) Florián, J.; Hrounda, V.; Hobza, P. *J. Am. Chem. Soc.* **1994**, *116*, 1457.
(21) Guallar, V.; Douhal, A.; Moreno, M.; Lluch, J. M. *J. Phys. Chem. A* **1999**, *103*, 6251.
(22) Shukla, M. K.; Leszczynski, J. *J. Phys. Chem. A* **2002**, *106*, 4709.
(23) Villani, G. *Chem. Phys.* **2005**, *316*, 1.
(24) Villani, G. *Chem. Phys.* **2007**, *336*, 143.
(25) Villani, G. *Chem. Phys. Phys. Chem.* **2010**, *12*, 2664.
(26) Perun, S.; Soboloewski, A. L.; Domcke, W. *J. Phys. Chem. A* **2006**, *110*, 9031.
(27) Ai, Y. J.; Zhang, F.; Cui, G. L.; Lio, Y.; Fang, W. H. *J. Chem. Phys.* **2010**, *133*, 064302.
(28) Roos, B. O. In *Advances in Chemical Physics; Ab Initio Methods in Quantum Chemistry II*; Lawley, K. P., Ed.; John Wiley & Sons Ltd.: Chichester, U.K., 1987; Vol. *399*.
(29) Andersson, K.; Malmqvist, P.-Å.; Roos, B. O. *J. Phys. Chem.* **1992**, *96*, 1218.
(30) Roos, B. O.; Fülscher, M. P.; Malmqvist, P.-Å.; Merchán, M.; Serrano-Andrés, L. In *Quantum Mechanical Electronic Structure with Chemical Accuracy, Understanding Chemical Reactions*; Langhoff, S. R., Ed.; Kluwer Academic Publishers: Dordretch, The Netherlands, 1995; Vol. *13*.
(31) Gobbo, J. P.; Borin, A. C.; Serrano-Andrés, L. *J. Phys. Chem. B* **2011**, *115*, 6243.
(32) Ghigo, G.; Roos, B. O.; Malmqvist, P.-Å. *Chem. Phys. Lett.* **2004**, *396*, 142.
(33) Forsberg, N.; Malmqvist, P.-Å. *Chem. Phys. Lett.* **1997**, *274*, 196.
(34) Pierloot, K.; Dumez, B.; Widmark, P.-O.; Roos, B. O. *Theor. Chim. Acta* **1995**, *90*, 87.
(35) Karlström, G.; Lindh, R.; Malmqvist, P.-Å.; Roos, B. O.; Ryde, U.; Veryazov, V.; Widmark, P.-O.; Cossi, M.; Schimmelpfennig, B.; Neogrady, P.; Seijo, L. *Comput. Mater. Sci.* **2003**, *28*, 222.
(36) Serrano-Andrés, L.; Borin, A. C.; Merchán, M. *Chem.—Eur. J.* **2006**, *12*, 6559.
(37) Malmqvist, P.-Å.; Pierloot, K.; Shahi, A. R. M.; Cramer, C. J.; Gagliardi, L. *J. Chem. Phys.* **2008**, *120*, 204109.
(38) Sauri, V.; Serrano-Andrés, L.; Shahi, A. R. M.; Gagliardi, L.; Vancoillie, S.; Pierloot, K. *J. Chem. Theory Comput.* **2011**, *7*, 153.